

Changes in ferromagnetic spin structure induced by exchange bias in Fe/MnF₂ filmsW. A. A. Macedo,^{1,2,*} B. Sahoo,³ V. Kuncser,^{3,†} J. Eisenmenger,^{1,‡} I. Felner,⁴ J. Nogués,⁵ Kai Liu,⁶ W. Keune,³ and Ivan K. Schuller¹¹Physics Department, University of California San Diego, La Jolla, California 92093, USA²Laboratório de Física Aplicada, Centro de Desenvolvimento da Tecnologia Nuclear, 30123-970 Belo Horizonte, Minas Gerais, Brazil³Institut für Physik, Universität Duisburg-Essen, D-47048 Duisburg, Germany⁴Racah Institute of Physics, The Hebrew University, Jerusalem 91904, Israel⁵Institució Catalana de Recerca i Estudis Avançats (ICREA) and Departament de Física, Universitat Autònoma de Barcelona, 08193 Bellaterra, Spain⁶Physics Department, University of California, Davis, California 95616, USA

(Received 15 September 2004; published 14 December 2004)

Depth-dependent Fe spin structures of the remanent state in exchange-coupled Fe/MnF₂ films have been probed using ⁵⁷Fe conversion electron Mössbauer spectroscopy, both above and well below the MnF₂ Néel temperature. ⁵⁷Fe probe layers were embedded either at the Fe/MnF₂ interface or in the center of the Fe film. Remarkably, exchange bias induces a significant change of the in-plane angular distribution of the Fe magnetic moments at the interface and inside the Fe film, away from the saturation magnetization direction. Results from vector magnetometry support these conclusions.

DOI: 10.1103/PhysRevB.70.224414

PACS number(s): 75.70.Cn, 75.30.Gw, 76.80.+y

I. INTRODUCTION

Exchange coupling between ferromagnet (F) and antiferromagnet (AF) films, often manifested in a shifted hysteresis loop away from zero field,¹ has been extensively studied due to its elusive mechanisms²⁻⁴ and important applications in spin-valve-type devices.⁵⁻⁷ Despite the intense research efforts, understanding the microscopic mechanisms of exchange bias (EB) has remained a challenging task.^{3,4,8-12} Of particular interest are the reversal processes occurring in low fields, indicative of the domain structures in the F and AF layers. While AF domains have been featured prominently in both theoretical¹³ and experimental¹⁴ studies, F domains have received much less attention.¹⁵ Two types of domain walls may form in the F during magnetization reversal: parallel and perpendicular to the interface. Because the *intraferromagnetic* layer interaction is presumably much stronger than the *interfacial* interaction, most models (except Ref. 3) neglect the F spin structure perpendicular to the interface (*z* direction). The depth dependence of the F or AF spin structures in EB systems is difficult to obtain experimentally. Only a limited number of techniques allow the study of buried magnetic interfaces, such as neutron diffraction,¹⁶ magnetic dichroism¹⁷ (or in conjunction with photoemission electron microscopy¹⁸), and conversion electron Mössbauer spectroscopy (CEMS).¹⁹ Studies of EB interfaces using these techniques are often challenging. For example, most low-angle neutron diffraction studies give no indication of structure in the F due to the AF,¹⁵ although some systems exhibit a depth-dependent magnetization profile²⁰ probably due to structural complications. Magnetic dichroism reveals thin interdiffused layers,^{14,21} together with the existence of uncompensated AF spins.^{14,22} Moreover, parallel¹⁴ and perpendicular²³ F-AF coupling were observed during reversal. Mössbauer studies of F-AF bilayers indicate in-plane F spins,²⁴ although out-of-plane F spin canting was also observed.²⁵

In this paper, we report on a depth-dependent Mössbauer study of the *effect of EB* on the spin structure of a F/AF system (Fe/MnF₂). By inserting a ⁵⁷Fe probe layer at different depth in the Fe layer and using CEMS, we have directly probed the remanent state Fe spin configurations, above and below the MnF₂ Néel temperature (*T_N*=67 K). Surprisingly, we find that, in remanence after zero-field cooling (ZFC), the F-layer spins reconfigure due to the AF ordering.

II. EXPERIMENTAL PROCEDURE AND RESULTS

Fe-MnF₂ and Fe-FeF₂ thin films have been extensively studied,^{2,15,26-28} thus providing an ideal system for this study. Multilayer samples of 30 Å Al cap / 70 Å Fe (60 Å natural Fe + 10 Å ⁵⁷Fe) / 520 Å MnF₂(110) / 160 Å ZnF₂(110) were grown on MgO(100) by electron beam evaporation.^{26,27} The ZnF₂ buffer layer was deposited at 200 °C, and the MnF₂ layer was evaporated at 2 Å/s and 325 °C.²⁶ The Fe (⁵⁷Fe and natural Fe) and the Al layers were deposited at 150 °C. A 10 Å ⁵⁷Fe probe layer was inserted either at the Fe-MnF₂ interface (interface sample), or in the center (center sample) of the Fe layer (35 Å away from the Fe/MnF₂ interface) using 95.5% enriched ⁵⁷Fe. Structural characterizations were performed by high-angle x-ray diffraction and grazing-incidence x-ray reflectivity (GIXR). The MnF₂ films are twinned quasiepitaxial with a (110) orientation, i.e., a compensated surface with the spins in the interface plane, and the Fe layers are polycrystalline. Besides the ⁵⁷Fe probe layer, our samples are comparable to those described earlier.^{26,27} As determined by GIXR (Fig. 1), the typical roughness at the Fe/MnF₂ interface is ~0.8 nm.

Magnetic hysteresis loops above and below the MnF₂ Néel temperature were measured using superconducting quantum interference device (SQUID) magnetometry (Fig. 2). EB was established by field cooling (FC) the samples in a *H*=2.0 kOe magnetic field applied in plane along the

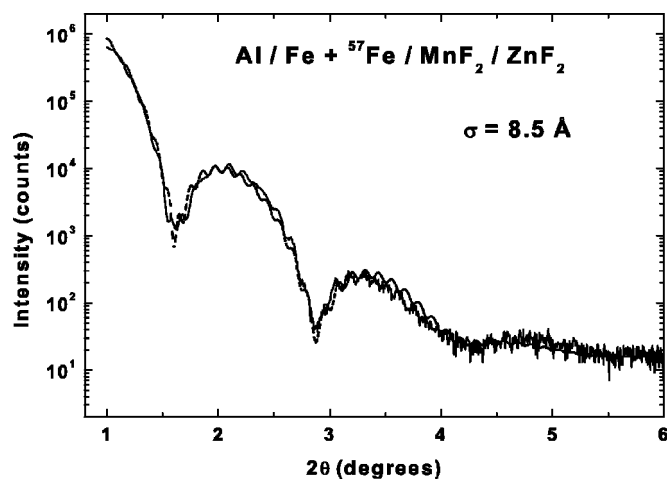


FIG. 1. Low-angle x-ray reflectivity data for the interface sample (solid line), along with the best least-squares fit (dashed line). The obtained Fe/MnF₂ interface roughness (rms value) is 8.5 Å.

MgO[001] direction, (*x* direction) from 150 K to below T_N . At 10 K, exchange fields H_E of -59 ± 2 and -55 ± 5 Oe were observed for the interface and center sample, respectively, consistent with previous results.²⁶ For CEMS, an alternative FC procedure was used: the samples were first saturated in an in-plane field of 4 kOe along MgO[001] at 300 K, then ZFC in remanence down to low T , and subsequently measured at $H=0$ Oe (“virgin” remanent state). The validity of this procedure was confirmed by similar FC and ZFC hysteresis loops at 10 K (e.g., $H_E = -54 \pm 2$ Oe for ZFC) for the interface sample, as shown in Fig. 2, also consistent with previous reports.²⁹ Moreover, for comparison with CEMS, the T dependence of the remanent magnetic moment components m_l (parallel to H and MgO[001]) and m_t (perpendicular to H and MgO[001]) of the center sample were measured by vector (SQUID) magnetometry at $H=0$ Oe during cooling in remanence (virgin remanent state). The results for m_l and

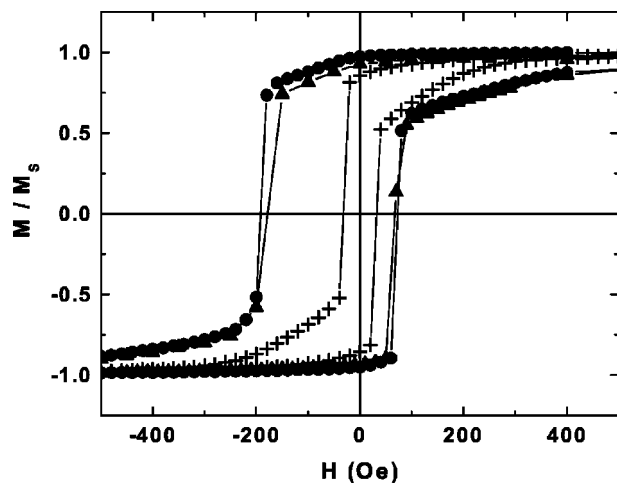


FIG. 2. SQUID hysteresis loops for the Fe+⁵⁷Fe / MnF₂(110) interface sample: field cooled, at 10 K (full circles) and at 80 K (crosses), and also at 10 K in the virgin remanent state (full triangles).

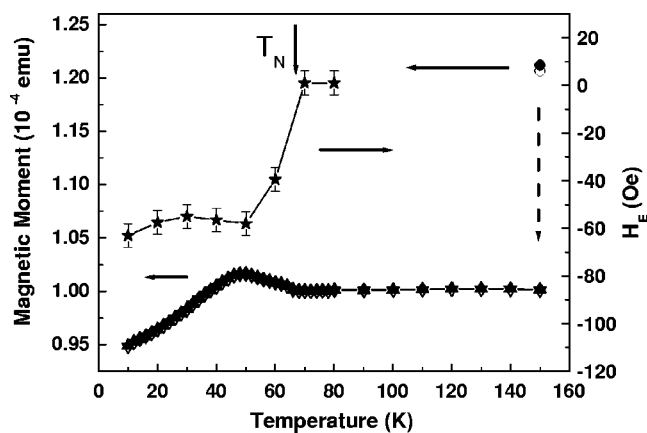


FIG. 3. T dependence of remanent m_l (open triangles) and m_{tot} (solid triangles) of the center sample measured for $H=0$ Oe during ZFC from 150 to 10 K. The prior saturation magnetization m_l (open circle) and m_{tot} (full circle) of the sample at $H=2$ kOe and 150 K is also shown. The exchange field H_E (also shown, asterisks) of the center sample was measured during warming up from 10 K after ZFC to 10 K.

total magnetic moment $m_{tot} = (m_l^2 + m_t^2)^{1/2}$ are shown in Fig. 3. The m_t values were found to be one order of magnitude smaller than m_l values, making m_l and m_{tot} comparable within the whole T range.

For low- T CEMS, we used a channel electron multiplier mounted inside a He cryostat, and a ⁵⁷Co source (Rh matrix). The CEMS spectra of the ⁵⁷Fe probe layer provide local (atomistic) information about the spontaneous angular spin orientation at various distances from the Fe-MnF₂ interface. By comparing the configurations above and below the T_N , we can distinguish the *change* of Fe spins caused by the MnF₂ ordering. At each T , the Fe spin configuration in the virgin remanent state (averaged over 10 Å in depth) is determined from the intensity ratio of the second (fifth) and the third (fourth) line, $R_{23} = I_2/I_3$, of the Zeeman-split Mössbauer sextet.^{19,30} If the magnetic hyperfine field (hf) B_{HF} (antiparallel to the Fe spin direction) at the ⁵⁷Fe nucleus forms an angle ψ with the Mössbauer γ -ray direction (cf. Fig. 4, top), then $R_{23} = 4 \sin^2 \psi / (1 + \cos^2 \psi)$.³⁰ In-plane spin configuration can only be probed with $\psi \neq 90^\circ$, e.g., when the γ ray incides at an angle ϕ with respect to the sample plane (Fig. 4, top). In the more general case, when the Fe spin direction has an angular distribution, $P(\varphi)$, in the sample plane [where φ is the azimuth angle relative to the saturation magnetization (M_s) axis x], the intensity ratio is given by³⁰

$$R_{23} = \int_0^{2\pi} \frac{1 - \cos^2 \phi \cos^2 \varphi}{1 + \cos^2 \phi \cos^2 \varphi} P(\varphi) d\varphi \quad \text{with} \quad \int_0^{2\pi} P(\varphi) d\varphi = 1.$$

Two simple models can be assumed for $P(\varphi)$: (i) all Fe spins point only in one direction (with $+\varphi$ and $-\varphi$ being equivalent); (ii) a steplike angular spin distribution, i.e., the Fe spins are uniformly distributed inside an aperture $\pm \Delta\varphi$ (relative to the M_s direction) in a fanlike manner. The orientation φ of the Fe spins in case (i), or the angular spin aperture $2\Delta\varphi$ in case (ii), may be obtained from the measured R_{23} ratio.³⁰

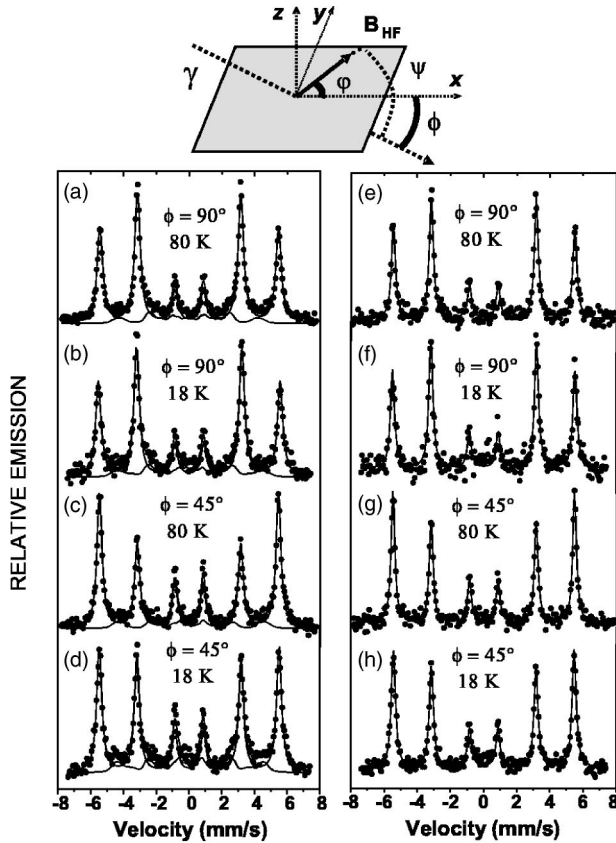


FIG. 4. Top: Schematic illustration of the CEMS geometry. Bottom: CEMS spectra of 10 Å ^{57}Fe probe layer at the Fe/MnF₂(110) interface for (a), (b) $\phi=90^\circ$ and (c), (d) $\phi=45^\circ$ geometries, at (a), (c) 80 K and (b), (d) 18 K. The corresponding CEMS spectra of a 10 Å ^{57}Fe probe layer at the center of the 70-Å-thick Fe film on MnF₂(110) are shown in (e)–(h).

Using the procedures just discussed, CEMS spectra were obtained with the γ ray perpendicular ($\phi=90^\circ$) and at an angle $\phi=45^\circ$ relative to the sample surface (xy plane) and to the M_s direction. The CEMS spectra of the interface sample are shown in Fig. 4 for the 90° and 45° geometries at (a) 80 and (b) 18 K for $\phi=90^\circ$, and at (c) 80 and (d) 18 K for $\phi=45^\circ$. The spectra were least-squares fitted with a pure α -Fe ($B_{HF}=33.9$ T at 18 K) dominant sextet and a weak component with a hf distribution (not shown) to account for the chemical intermixing at the very Fe-MnF₂ interface. At $\phi=90^\circ$, the best fits of the spectra were obtained for an intensity ratio $R_{23}=4.0$ for both subspectra at 80 and 18 K, implying that the Fe spins of the ^{57}Fe layer rest entirely in plane. At $\phi=45^\circ$ [Figs. 4(c) and 4(d)], there is an obvious change of the R_{23} ratio with T : $R_{23}=1.9(1)$ at 80 K, increas-

ing to $R_{23}=2.7(1)$ at 18 K. Note that for unidirectional (or uniaxial) spin orientation, along the remanent magnetization (RM) direction, i.e., for $\psi=\phi=45^\circ$ and $\varphi=0^\circ$, the theoretical R_{23} value of $4/3=1.33$ (Ref. 30) is much lower than the measured value. The weak interfacial contribution (of only $\sim 15\%$ of the total integrated intensity and same R_{23} ratio as the α -Fe sextet) does not affect in any way the conclusions of this paper and, therefore, is not further discussed.

CEMS spectra for the center sample are shown in Figs. 4(e)–4(h) and were least-squares fitted with a α -Fe sextet. For perpendicular incidence [Figs. 4(e) and 4(f)], the measurements again give $R_{23}=4.0$, indicating complete in-plane Fe spin alignment in the centered ^{57}Fe probe layer. For $\phi=45^\circ$, $R_{23}=2.3(1)$ at 80 K [Fig. 4(g)], and $R_{23}=2.6(1)$ at 18 K [Fig. 4(h)]. Note that at 18 K, below T_N , the R_{23} ratio is essentially the same as that of the interface sample, whereas at 80 K, above T_N , their R_{23} values are different.

III. DISCUSSION

The changes of R_{23} upon cooling from 80 to 18 K show that the EB induces a significant in-plane rotation of the Fe spins, which causes an angular change $\Delta\psi$ between the γ -ray direction and the *average* orientation of the Fe spins (or of B_{HF}) of $\sim 11^\circ$ and $\sim 4^\circ$ at the interface and the center of the Fe layers, respectively. The observed changes of R_{23} on cooling the interface sample to 18 K are consistent either (i) with a uniform (unidirectional or bidirectional) in-plane rotation of unidirectionally aligned interfacial Fe spins by a difference in angle [$\varphi(18\text{ K})-\varphi(80\text{ K})$] of 20° away from the RM direction, or (ii) with an increase of [$2\Delta\varphi(18\text{ K})-2\Delta\varphi(80\text{ K})$] by 90° of the interfacial in-plane Fe spin fanning away from the RM (x) direction. For the center sample, although it shows a smaller change in R_{23} on cooling below T_N , the R_{23} value at 18 K indicates a similar Fe spin structure to that of the interface sample. Thus, the remanent F spin structure in the EB state is similar, at or away from the F-AF interface. Our results are summarized in Table I.

At 80 K, above T_N , the difference in R_{23} between the center and interface samples (Table I) could be attributed to the different remanent domain configurations, caused by small variations in sample microstructures (evidenced by small differences in H_E). However, after EB is established below T_N , the Fe spins in both samples rearrange themselves to a very similar configuration. In twinned MnF₂(110) on MgO(100) the easy axes of the MnF₂ domains are oriented such that $[110]\text{MnF}_2 \parallel [110]\text{MgO}$ or $[001]\text{MnF}_2 \parallel [110]\text{MgO}$. Thus the MnF₂ spins are at $\pm 45^\circ$ with the Fe M_s direction along $[001]\text{MgO}$, as illustrated in Fig. 5(a).

TABLE I. R_{23} ratio and the corresponding angles φ , $2\Delta\varphi$, and ψ (in degrees) for the interface and center samples at the $\phi=45^\circ$ geometry, above (80 K) and well below (18 K) T_N .

T (K)	Interface sample				Center sample			
	R_{23}	φ	$2\Delta\varphi$	ψ	R_{23}	φ	$2\Delta\varphi$	ψ
80	1.9(1)	32	110	53	2.3(1)	42	160	59
18	2.7(1)	52	200	64	2.6(1)	50	185	63

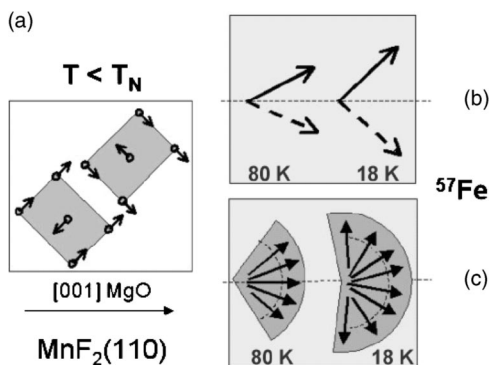


FIG. 5. Schematic drawing illustrating (a) the AF spin structure in twinned MnF₂(110), and the in-plane Fe spin configuration estimated from the (b) uniform spin-rotation ($\pm\varphi$) and (c) spin-fanning ($2\Delta\varphi$) model, respectively. Results in (b) and (c) are for the interface sample at 80 and 18 K.

The present results demonstrate that due to the exchange coupling with the MnF₂ spins, independent of the model used, the Fe spins in the virgin remanent state reorient towards the AF spin directions, which are at $\pm 45^\circ$ relative to the MgO[001] direction. Schematic illustrations of this reorientation are shown in Figs. 5(b) and 5(c) for rotation (two equivalent directions) and fanning, respectively.³¹

Our conclusions from CEMS are supported by the T dependence of m_l and m_{tot} for the center sample (Fig. 3). Upon ZFC from 150 K, m_l and m_{tot} first remain constant down to $T_N=67$ K, then show a maximum at ~ 49 K (whose origin is not yet understood), followed by a significant decrease on cooling to 10 K. The decrease of m_l and m_{tot} is the indication of rotation (or fanning) away from the MgO[001] direction due to EB, in accordance with CEMS. Moreover, the observed very small m_t suggests that (averaged over the entire sample) this rotation or fanning is bidirectional, i.e., symmetrical with respect to the MgO[001] axis. After ZFC to 10 K, we measured sequentially the following values: $m_l=0.9482(2)\times 10^{-4}$ emu at $H=0$ Oe (virgin remanence), $m_{sat}=1.234(104)\times 10^{-4}$ emu (saturation moment) by applying $H=2$ kOe and then $m_l=1.106(4)\times 10^{-4}$ emu (conventional remanence) again at $H=0$ Oe. Note that there is a $\sim 16\%$ difference between m_l at virgin and conventional remanence. Using these m_l values, a simple calculation al-

lows us to estimate the bidirectional rotation (or fanning) angles φ (or $\Delta\varphi$) for the center sample at 10 K, as follows: $\varphi=\pm 40^\circ$ ($\Delta\varphi=\pm 70^\circ$) at virgin remanence, being in fair agreement with CEMS results at 18 K (Table I, center sample), and $\varphi=\pm 26^\circ$ ($\Delta\varphi=\pm 42^\circ$) at conventional remanence.

IV. SUMMARY

We have used CEMS to determine the spin structure of ⁵⁷Fe probe layers embedded in a Fe layer exchange coupled to a twinned MnF₂(110) layer. The change of the Mössbauer line intensity ratio R_{23} below T_N demonstrates in a model free way that, in remanence, EB induces a significant change of the in-plane angular spin distribution of the Fe spins. In particular, the Fe spins orient bidirectionally towards the MnF₂ spin directions, which are at $\pm 45^\circ$ relative to the MgO[001] direction. Our observations are corroborated by vector magnetometry of the remanent m_l and m_t . After the exchange coupling is established, the resulting Fe spin structure at the interface is similar to that in the center of the Fe film. Out-of-plane Fe spin canting in the Fe/MnF₂(110) bilayers is ruled out.²⁵ It has been proposed¹⁵ for Fe on twinned MnF₂(110) and twinned FeF₂(110) that the MgO[001] direction between the $\pm 45^\circ$ AF spin directions constitute an easy axis for the Fe magnetization below T_N , due to frustration of the perpendicular coupling³² between AF and F spins in a twinned system. Our results demonstrate, however, that microscopically, in the *remanent state* below T_N , the Fe spins rotate (or fan) spontaneously *away* from this easy direction. We speculate that fanning at remanence might occur as the result of competing interactions (perpendicular coupling, dipolar interactions) in a twinned system.

ACKNOWLEDGMENT

We acknowledge the support by the U.S.-D.O.E., the U.S.-Israel BSF, the DFG (SFB-491), the CNPq (Brazil), the AvH Foundation, the Spanish CICYT (MAT2001-2555), and the Catalan DGR (2001SGR00189). W.A.A.M. gratefully acknowledges the hospitality during his stay at the UCSD, and thanks J. Santamaria and R. Paniago for assistance with GIXR simulations.

*Electronic address: wmacedo@cdtn.br

†Permanent address: National Institute of Physics of Materials, RO-76900 Bucharest-Magurele, Romania.

‡Present address: Abteilung Festkörperphysik, Universität Ulm, D-89069 Ulm, Germany.

¹W. H. Meiklejohn and C. P. Bean, Phys. Rev. **102**, 1413 (1956).

²J. Nogués and I. K. Schuller, J. Magn. Magn. Mater. **192**, 203 (1999).

³M. Kiwi, J. Mejía-López, R. D. Portugal, and R. Ramírez, Europhys. Lett. **48**, 573 (1999).

⁴R. L. Stamps, J. Phys. D **33**, R247 (2000).

⁵B. Dieny, V. S. Speriosu, S. S. P. Parkin, B. A. Gurney, D. R. Wilhoit, and D. Mauri, Phys. Rev. B **43**, R1297 (1991).

⁶J. S. Moodera, T. H. Kim, C. Tanaka, and C. H. Degroot, Philos. Mag. B **80**, 195 (2000).

⁷J. M. Daughton, A. V. Pohm, R. T. Fayfield, and C. H. Smith, J. Phys. D **32**, R169 (1999).

⁸D. Mauri, H. C. Siegmann, P. S. Bagus, and E. Kay, J. Appl. Phys. **62**, 3047 (1987).

⁹A. P. Malozemoff, Phys. Rev. B **35**, R3679 (1987).

¹⁰N. C. Koon, Phys. Rev. Lett. **78**, 4865 (1997).

¹¹T. C. Schulthess and W. H. Butler, Phys. Rev. Lett. **81**, 4516

- (1998).
- ¹²P. Miltényi, M. Gierlings, J. Keller, B. Beschoten, G. Güntherodt, U. Nowak, and K. D. Usadel, *Phys. Rev. Lett.* **84**, 4224 (2000).
- ¹³B. Beckmann, U. Nowak, and K. D. Usadel, *Phys. Rev. Lett.* **91**, 187201 (2003).
- ¹⁴H. Ohldag, T. J. Regan, J. Stöhr, A. Scholl, F. Nolting, J. Lüning, C. Stamm, S. Anders, and R. L. White, *Phys. Rev. Lett.* **87**, 247201 (2001).
- ¹⁵M. R. Fitzsimmons, P. Yashar, C. Leighton, I. K. Schuller, J. Nogués, C. F. Majkrzak, and J. A. Dura, *Phys. Rev. Lett.* **84**, 3986 (2000).
- ¹⁶H. Zabel, R. Siebrecht, and A. Schreyer, *Physica B* **276**, 17 (2000).
- ¹⁷J. B. Kortright, D. D. Awschalom, J. Stöhr, S. D. Bader, Y. U. Idzerda, S. S. P. Parkin, I. K. Schuller, and H. C. Siegmann, *J. Magn. Magn. Mater.* **207**, 7 (1999).
- ¹⁸B. P. Tonner, D. Dunham, T. Droubay, J. Kikuma, and J. Denlinger, *J. Electron Spectrosc. Relat. Phenom.* **78**, 13 (1996).
- ¹⁹T. Shinjo and W. Keune, *J. Magn. Magn. Mater.* **200**, 598 (1999).
- ²⁰A. R. Ball, A. J. G. Leenaers, P. J. van der Zaag, K. A. Shaw, B. Singer, D. M. Lind, H. Fredrikze, and M. Th. Rekveldt, *Appl. Phys. Lett.* **69**, 583 (1996).
- ²¹A. D. Alvarenga, F. Garcia, W. D. Brewer, M. Gruyters, M. Gierlings, M. S. Reis, P. Panissod, L. C. Sampaio, and A. P. Guimarães, *J. Magn. Magn. Mater.* **242**, 958 (2002).
- ²²W. J. Antel Jr., F. Perjeru, and G. R. Harp, *Phys. Rev. Lett.* **83**, 1439 (1999).
- ²³H. Matsuyama, C. Haginoya, and K. Koike, *Phys. Rev. Lett.* **85**, 646 (2000).
- ²⁴R. Jungblut, R. Coehoorn, M. T. Johnson, Ch. Sauer, P. J. van der Zaag, A. R. Ball, Th. G. S. M. Rijks, J. aan de Stegge, and A. Reinders, *J. Magn. Magn. Mater.* **148**, 300 (1995).
- ²⁵I. L. Siu, M. N. Islam, and J. C. Walker, *J. Appl. Phys.* **88**, 5293 (2000).
- ²⁶C. Leighton, J. Nogués, H. Suhl, and I. K. Schuller, *Phys. Rev. B* **60**, 12 837 (1999).
- ²⁷I. N. Krivorotov, C. Leighton, J. Nogués, I. K. Schuller, and E. D. Dahlberg, *Phys. Rev. B* **68**, 054430 (2003).
- ²⁸M. Grimsditch, A. Hoffmann, P. Vavassori, H. Shi, and D. Lederman, *Phys. Rev. Lett.* **90**, 257201 (2003).
- ²⁹P. Miltényi, M. Gierlings, M. Bammig, U. May, G. Güntherodt, J. Nogués, M. Gruyters, C. Leighton, and Ivan K. Schuller, *Appl. Phys. Lett.* **75**, 2304 (1999).
- ³⁰V. Kuncser, W. Keune, M. Vopsaroiu, and P. R. Bissel, *Nucl. Instrum. Methods Phys. Res. B* **196**, 135 (2002).
- ³¹Simulations for spin fanning around $\varphi = \pm 45^\circ$ (the AF spin axes) show a minimum R_{23} value of 2.40 when $\Delta\varphi = 0^\circ$ (uniform rotation), and a maximum R_{23} value of 2.56 when the fanning aperture $\Delta\varphi = \pm 66^\circ$. This last $\Delta\varphi$ value corresponds to an in-plane angular interval $\Delta\varphi = \pm 111^\circ$ with respect to the x axis, or a total aperture $2\Delta\varphi = 222^\circ$, in fair agreement with the $2\Delta\varphi$ values at 18 K given in Table I.
- ³²T. J. Moran, J. Nogués, D. Lederman, and I. K. Schuller, *Appl. Phys. Lett.* **72**, 617 (1998).